Toxicology Reports 8 (2021) 627–635

Contents lists available at ScienceDirect

Toxicology Reports

journal homepage: www.elsevier.com/locate/toxrep

A novel 3D polycaprolactone high-throughput system for evaluation of toxicity in normoxia and hypoxia

Atena Malakpour-Permlid, Stina Oredsson *

Department of Biology, Lund University, Lund, Sweden

ARTICLE INFO

Edited by Dr. A.M Tsatsaka

Keywords:
3D high-throughput screening
Polycaprolactone fibre network
Breast cancer cells
Paclitaxel
Multi-well plates
Hypoxia

ABSTRACT

Two-dimensional (2D) culturing of cancer cells has been indispensable for the development of anti-cancer drugs. Drug development, however, is lengthy and costly with a high attrition rate, calling to mind that 2D culturing does not mimic the three-dimensional (3D) tumour microenvironment *in vivo*. Thus, began the development of 3D culture models for cancer research. We have constructed a 3D 96-well plate using electrospun fibres made of biocompatible polycaprolactone (PCL). Finely-cut PCL fibre pieces in water/ethanol solution was pipetted to the wells of hydrophobic 96-well plates. A fibrous network of approximately 200 μm thickness and high porosity was formed after crosslinking and drying. Human JIMT-1 breast cancer cells or fibroblasts were seeded into the network. Confocal microscopy shows that the cells grow throughout the fibre network. The toxicity of paclitaxel and an experimental salinomycin analogue was assessed and compared in 2D and 3D cultures incubated under conditions of normoxia and hypoxia often found in tumours. The toxicity of both compounds is lower when the cells are cultured in 3D compared to 2D in either normoxia or hypoxia. We conclude that our 96-well assay is a cost-efficient tool that may be used for high-throughput pre-clinical screening of potential anti-cancer compounds.

1. Introduction

The high-throughput screening (HTS) concept in drug discovery using microtiter plates was introduced in 1986 [1]. Before too long, HTS was applied to two-dimensional (2D) cell cultures in multi-well settings to efficiently screen thousands of compounds for the discovery of chemical compounds in the search for new drug candidates. 2D cell culturing has without doubt resulted in a wealth of valuable insight and information contributing to the understanding of the mechanism of action and toxicity of chemical compounds that potentially could be used in the treatment of various diseases. At the same time, it is well known that the pre-clinical drug discovery process is a slow and costly business and it's high attrition rate has partly been attributed to the morphological and functional difference between 2D cell culturing of single cell types grown on planar rigid plastic surfaces compared to the three-dimensional (3D) structure in the human body. As a result, significant efforts have been put into developing 3D cell cultures that can be used as tools in early drug development stages during the last two decades. The scientific basis of this work is the realization that 2D cell culturing lacks the *in vivo* tissue-specific architecture with cell-to-cell and cell-to-matrix communications, including mechanical and biochemical cues involved in these interactions [2,3].

A wide range of 3D cell culture technologies for drug discovery are under development including multicellular spheroids, organoids, scaffolds, hydrogels, organs-on-chips, and 3D bioprinting [4]. One important aspect of 3D cultures is the consideration of the extracellular matrix (ECM) as a crucial feature in the formation of a 3D cellular organization and structure similar to the properties of the microenvironment *in vivo* [5]. Scaffold-based 3D cultures made of natural or synthetic materials can be used to ensure cell-to-cell contact, ECM deposition, proliferation, 3D morphology, and polarization of the cells [6]. On the other hand, scaffold-free 3D cell cultures rely on the self-aggregation of cells by the contribution of their own secreted ECM. 3D multicellular spheroids and organoids have so far been successfully used for screening of large libraries of chemical compounds [7,8]. However, there is ongoing discussions concerning the efficiency of the application of spheroids and organoids in HTS but also the limitations related to consistency in size and morphology, robustness, labour intensity, and time consumption [9,

Abbreviations: 2D, two-dimensional; 3D, three-dimensional; CSCs, cancer stem cells; DHHS, donor herd horse serum; ECM, extracellular matrix; FBS, fetal bovine serum; HDFs, human dermal fibroblasts; HTS, high-throughput; PCL, polycaprolactone; SAEC, salinomycin analogue 20-ethyl carbonate-Na.

* Corresponding author at: Department of Biology, Lund University, Sölvegatan 35C, 223 62, Lund, Sweden.
E-mail address: stina.oredsson@biol.lu.se (S. Oredsson).

https://doi.org/10.1016/j.toxrep.2021.03.015
Received 11 November 2020; Received in revised form 12 March 2021; Accepted 18 March 2021
Available online 20 March 2021

10]. Therefore, the development and application of robust HTS 3D cell culturing still remains a challenge. So far, there has been no 3D system that seems to "fit all" in the same manner as 2D cell culturing has been used in HTS drug discovery. Neither are there any 3D HTS assays yet that have been proven to predict *in vivo* toxicity and at the same time be truly biologically relevant. Thus, there is room for more ideas to be exploited in the search for an optimal 3D HTS assay that will result in better pre-clinical drug prediction than is obtained today.

Many of the scaffold-based 3D assays utilize natural products derived from animals such as collagen, gelatine, and Matrigel™, which are ethically questionable [11]. In addition, these components display large batch-to-batch variations, which is specifically apparent regarding Matrigel™ owing to its complex, ill-defined, and variable composition [12]. We have utilized biocompatible electrospun polycaprolactone (PCL) fibres as a 3D scaffold for formation of 3D mono-cultures of cancer cells or fibroblasts [13,14] and also 3D co-cultures of cancer cells and fibroblasts [15]. However, our previously investigated 3D scaffold structures cannot be down-scaled to be used in multi-well plates. To address this, we decided to develop a 96-well plate with a 3D PCL-based fibre network that can be produced without advanced instruments or expertise in a cost-efficient manner. In the present study, we compare the toxicity of paclitaxel and a salinomycin analogue in JIMT-1 breast cancer cells and human dermal fibroblasts (HDFs) grown in conventional 2D 96-well plates and in our 3D PCL-based 96-well plate incubated under both normoxic and hypoxic conditions. We included hypoxic conditions for two reasons. Firstly, it is well known that tumours contain regions of hypoxia and that they contribute to drug resistance [16,17; Trédan et al., 2007]. Secondly, knowing this fact, there is surprisingly scarce information about HTS of anti-cancer drugs in hypoxia. The JIMT-1 cancer cells and HDFs show differential toxicity in response to the compounds in cultures incubated in normoxia or hypoxia, where cells in 2D cultures are more sensitive to treatments compared to those in 3D cultures under both conditions. We believe that this 3D 96-well assay can complement and contribute to better selection of potential anti-cancer drugs compared to the 2D HTS assays used today.

2. Materials and methods

2.1. Electrospinning of aligned PCL fibres

The PCL fibres were prepared according to Jakobsson et al. [13], however, using a rotating collector. The biocompatibility of the fibres is investigated and discussed in Malakpour-Permlid et al. [14]. The mean fibre diameter size obtained is 500 nm [13]. In short, a 15 % PCL solution was prepared by dissolving PCL pellets (80 kDa) (Sigma-Aldrich Sweden AB, Stockholm, Sweden) in acetone overnight at room temperature. The electrospinning process was performed horizontally using a syringe pump (Aladdin-1000, World Precision Instruments, Sarasota, FL, USA) set at a continuous flow rate of 2.0 mL/h, a high voltage power supply (+16 kV) (FuG Elektronik GmbH, Schechen, Germany), and a blunt needle tip-collector at a distance of 20 cm. The aligned fibres were deposited and collected on a rotating collector with 15 cm diameter and a controllable rotation speed of 1500 rotations per minute at room temperature.

2.2. Preparation of polycaprolactone 3D meshes in 96-well plates

The electrospun PCL fibres were kept at −80 °C. Also, a mixture of 99.6 % ethanol and Millipore water (2:1) was stored at −80 °C. The PCL fibres were quickly cut into smaller pieces and mixed into the semi-solid ethanol/water mix at a concentration of 4 mg PCL fibre per ml solution. The mixture was stored at −80 °C overnight. The semi-solid PCL ethanol/water mixture was scoped into the sterilized Waring LB20ES laboratory mixer (Radnor, PA, USA) placed in a laminar air flow (LAF) bench. The cutting process was performed at maximum speed for 15 min. At approximately 3 min intervals, the mixer was stopped and liquid nitrogen added (10 mL per 100 mL mixture). The purpose of the liquid nitrogen addition was to keep the temperature of the mixture below −60 °C, the glass transition point of PCL. Then, the solution was removed from the blender to a reservoir. A multi-pipette was used to pipette 150 µL of the solution to the wells of round-bottomed hydrophobic 96-well plates (Nunc, Roskilde, Denmark) only filling rows B–G and columns 1–11. The plates were then incubated without the lids at 59 °C for 7 min and immediately placed on ice afterwards. The plates were then allowed to dry in a LAF bench. The PCL mesh-incorporated 96-well plates were subjected to O_2 plasma treatment for 10 s in a ZEPTO low-pressure plasma laboratory unit (Diener electronic GmbH Co., Ebhausen, Germany) to obtain hydrophilic fibres [14]. Then, the plates were sterilized in 99.6 % ethanol for 15 min and they were then rinsed three times with sterile phosphate-buffered saline (PBS) before seeding cells.

2.3. Scanning electron microscopy

After preparation and O_2 plasma treatment, 3D PCL fibre meshes from different 96-well plates were extracted from the wells and subjected to dehydration in an hexamethyldisilane (HMDS) series (25 %, 50 %, 75 %, and 100 %) for 15 min in each step. Then, they were left to dry at room temperature overnight before mounting on aluminium stubs using adhesive carbon tape. The samples were then sputter-coated with a thin layer of gold using a Cressington 108auto sputter coater (Cressington Scientific Instruments Ltd.) for 55 s at 20 mA. The 3D fibre meshes were visualized with a scanning electron microscope (SEM) (Model SU3500, Hitachi, Krefeld, Germany) and images were captured at an accelerating voltage of 5 kV. Three replicates were imaged and 3–5 images taken per replicate.

2.4. Cell lines

The human breast carcinoma cell line JIMT-1 was purchased from the German Collection of Microorganisms and Cell Cultures (Braunschweig, Germany). The cells were tested for mycoplasma during the experimental period and were found to be negative (Eurofins Scientific, Cologne, Germany). HDFs were purchased from Sigma-Aldrich Sweden AB (Stockholm, Sweden). The HDFs were maximally used for up to 7 passages. The cell lines were cultured in Dulbecco's modified Eagle medium/Ham's F-12 (1:1) supplemented with 5 % heat-inactivated donor herd horse serum (DHHS) (Sigma-Aldrich Sweden AB), 5 µg/mL insulin (Sigma-Aldrich Sweden AB), 10 ng/mL epidermal growth factor (Lonza, Basel, Switzerland), 0.5 µg/mL hydrocortisone (Sigma-Aldrich Sweden AB), 1 mM Na-pyruvate (Sigma-Aldrich Sweden AB), 50 µg/mL transferrin (Sigma-Aldrich Sweden AB), 2 mM L-glutamine (VWR, Lund, Sweden), 1 mM non-essential amino acids (VWR), 100 µg/mL streptomycin (VWR), and 100 U/mL penicillin (VWR). The cell lines were maintained in a humidified incubator (95 % humidity) with 5 % CO_2 in air at 37 °C (CO_2 incubator). The cells were passaged twice a week using Accutase™ (Sigma-Aldrich Sweden AB).

2.5. Compounds for treatment

The salinomycin analogue 20-ethyl carbonate-Na (SAEC) was kindly provided by Björn Borgström and Daniel Strand at the Centre for Analysis and Synthesis, Department of Chemistry, Lund University [18,19]. SAEC was used because of its higher toxicity and anti-cancer stem cell specificity compared to the mother compound salinomycin [18,19]. A 10 mM stock solution was made in 100 % dimethyl sulfoxide (DMSO), which was stored at −20 °C. A serial dilution using PBS with 5000, 2500, 1000, 500, 10, 50, and 10 nM concentrations was prepared and used. The conventional chemotherapeutic drug, paclitaxel was obtained from Tocris Bioscience (Abingdon, United Kingdom). A 100 mM stock solution was made in 100 % DMSO which was stored at −20 °C. A serial dilution using PBS with 8000, 2000, 500, 125, 31.2, 0.78, and 0.19 nM concentrations was prepared and used.

2.6. Dose response assay

The cells were detached using Accutase™ Sigma-Aldrich Sweden AB (Stockholm, Sweden) and counted in a hemocytometer. Cell suspensions were made with 7000 cells per 180 μL growth medium (2D cell culturing) and 21,000 cells per 180 μL growth medium (3D cell culturing). The cell suspensions were added to the custom-made 3D PCL-based 96-well plates and to conventional flat-bottomed 96-well 2D plates (Nunc, Roskilde, Denmark). The plates were incubated for 24 h before addition of the compounds at the concentrations described above. The compounds were added in 20 μL aliquots resulting in 10 times dilutions. Control wells received PBS with 0.05 % DMSO for SAEC and 0.008 % DMSO for paclitaxel yielding final DMSO concentrations of 0.005 % and 0.008 % DMSO, respectively. The plates were then transferred to the regular CO_2 incubator (5 % CO_2 and 18 % O_2 in air) [20] or to a hypoxia station Don Whitley Hypoxia station (Don Whitley Scientific, Victoria Works, United Kingdom) set at 1 % O_2 [21]. After 72 h of incubation, MTT solution was added (Sigma-Aldrich Sweden AB: 20 μL of 5 mg/mL MTT in PBS) and the plates incubated for 2 h. The MTT containing medium was removed and DMSO was added to the plates (100 μL/well for 2D plates and 150 μL/well for 3D plates). The plates were shaken on a lab shaker protected from light. The absorbance in the 2D plates was measured after 15 min of incubation. The 3D plates were shaken for 2 h to dissolve all formazan crystals in the 3D mesh. Then, 100 μL of the DMSO solution with dissolved formazan was transferred to a flat-bottomed 96-well plate and the absorbance was measured at 540 nm in a Multiskan™ FC Microplate Photometer (Thermo Fisher Scientific, Lund, Sweden) using the software SkanIt 3.1. Background was obtained from 2D flat wells and 3D wells with fibre mesh that did not contain cells. This background was subtracted from all values obtained from wells with cells. At least three experiments were performed for each condition with 3–6 wells per concentration (a total of n = 12–18 for each concentration from three experiments). GraphPad Prism version 8 (GraphPad Software, La Jolla, CA, USA) was used for drawing dose response curves and calculating the IC_{50} values, *i.e.* the dose giving 50 % reduction in MTT readout which is supposed to reflect a 50 % reduction in cell number.

2.7. Cells for confocal microscopy imaging

JIMT-1 cells and HDFs were also seeded in 3D 96-well plates for confocal microscopy imaging as described above for the dose response curve assay. In addition, we co-seeded 15,000 JIMT-1 cells and 15,000 HDFs in 180 μL medium to obtain co-cultures. These cultures were fixed in 3.7 % formaldehyde at 4 days after seeding *i.e.* they were equivalent to the controls used in the MTT dose response assays.

2.8. Staining of cultures

The fixed cultures were washed three times with PBS before blocking and permeabilization with blocking buffer (1 % bovine serum albumin and 1 % Tween 20 in PBS) at room temperature for 1 h. For the labelling, different antibodies were used. To label CD44 on JIMT-1 cells, the primary rabbit anti-CD44 antibody (ab189524, 1:300) (Abcam, Cambridge, United Kingdom) was used. HDFs in mono- and co-cultures were stained with the primary mouse anti-vimentin antibody (ab8069, 1:500) (Abcam, Cambridge, United Kingdom). Vimentin was used to distinguish JIMT-1 cells from the HDFs in co-cultures. The samples were incubated overnight at 4 °C with the primary antibody followed by washing three times with PBS, and incubation for 2 h at room temperature with the secondary antibody Alexa Flour™ 594 goat anti-rabbit (A11037, 1:600) (ThermoFisher Scientific, Waltham, MA, USA) or Alexa Flour™488 goat anti-mouse (A11029, 1:1000) (ThermoFisher Scientific, Waltham, MA, USA). Then, the cultures were washed three times with PBS and the cell nuclei were stained with 4′,6-diamidino-2-phenylindole (DAPI) (1 μg/mL PBS) (ThermoFisher Scientific, Waltham, MA, USA) for 2 min at room temperature.

2.9. Confocal microscopy

The stained samples were mounted with RapiClear® 1.49 clearing agent (10 μL) (SunJin Lab Co., Hsinchu, Taiwan) on glass cover and images were taken with Leica SP8 DLS inverted confocal laser scanning microscope (Leica Microsystems, Wetzlar, Germany) using 20×/0.75 IMM oil immersion objective. At least three replicates were imaged for each culture condition and 3–7 images taken per replicate.

3. Results

3.1. Characterization of the PCL fibre network

We aimed to create an HTS-compatible 3D 96-well plate that can replace the standard 2D 96-well plate for cytotoxicity evaluation of compounds and that can be fabricated in any standard cell culturing laboratory to a low cost. Fig. 1A shows the polystyrene round-bottomed 96-well plate with incorporated 3D PCL fibre networks. Due to the hydrophobic nature of PCL, the plates were subjected to O_2 plasma treatment before seeding to obtain hydrophilic PCL fibres to allow efficient attachment [14]. Similar to conventional 2D cell seeding in 96-well plates, the cells were seeded in columns 2–11, rows B–H. The 3D PCL network wells in column 1 containing only media is used for background correction.

The PCL fibre network in the 96-well plates was fabricated by adding a solution of finely-cut PCL fibres in ethanol/water to the wells, thermally-crosslinking the fibres, and drying at room temperature afterwards. SEM was used to investigate the topography and distribution of the 3D fibre network and also to evaluate the pore size of the 3D network (Fig. 1B). SEM analysis revealed different PCL fibre morphology including larger fibres as well as densely packed areas with thin fibrils that form the network. The mean pore area is approximately 50 μm^2. The thickness of the native fibre network without cells is around 200 μm (206 μM ± 19 (SEM) for n = 12 images from 3 replicates) (Fig. 1C).

3.2. Morphology and distribution of cells in the HTS PCL fibre network

First, we studied the morphology, distribution, and infiltration of the cells in the 3D HTS fibre network 96 h after seeding. 3D fibre networks with non-treated cells were removed from the wells and were viewed in the confocal microscope after fixation and labelling/staining (Fig. 2). The cells were detected by immunostaining with specific markers for cancer cells and HDFs, *i.e.* CD44 and vimentin, respectively. In addition, we decided to co-culture JIMT-1 cells and HDFs to analyse the possibility of using the 3D 96-well plates in order to recreate a more tumour realistic setting. However, we have not performed MTT assays on co-cultures as the readout does not distinguish between treatment effects on the different cell types and it needs to be further optimized. Fig. 2 shows images taken in the centre of 3D fibre networks extracted from 96-well plates. As shown previously, the JIMT-1 cells are found growing in tight clusters of different sizes while the HDFs spread out along the PCL fibre network in both normoxia and hypoxia [14]. When co-cultured, the JIMT-1 cancer cells grow in irregular clusters surrounded by the fibroblasts in 3D fibre networks incubated in either normoxia or hypoxia (unpublished results). This growth pattern has been observed previously by Jaganathan et al. [22].

Confocal microscopy z stack imaging shows distribution and infiltration of cells throughout a depth of approximately 100 μm in the 3D fibre network 96 h after seeding. Fig. 3 shows seven confocal plane images taken at different z levels of JIMT-1 cells grown in 3D cultures in normoxia (Fig. 3A) or hypoxia (Fig. 3B) indicating the depth of the 3D culture. Therefore, the HTS PCL fibre network with a mean pore size of 50 μm, provides adequate spacing and porosity for cell penetration and

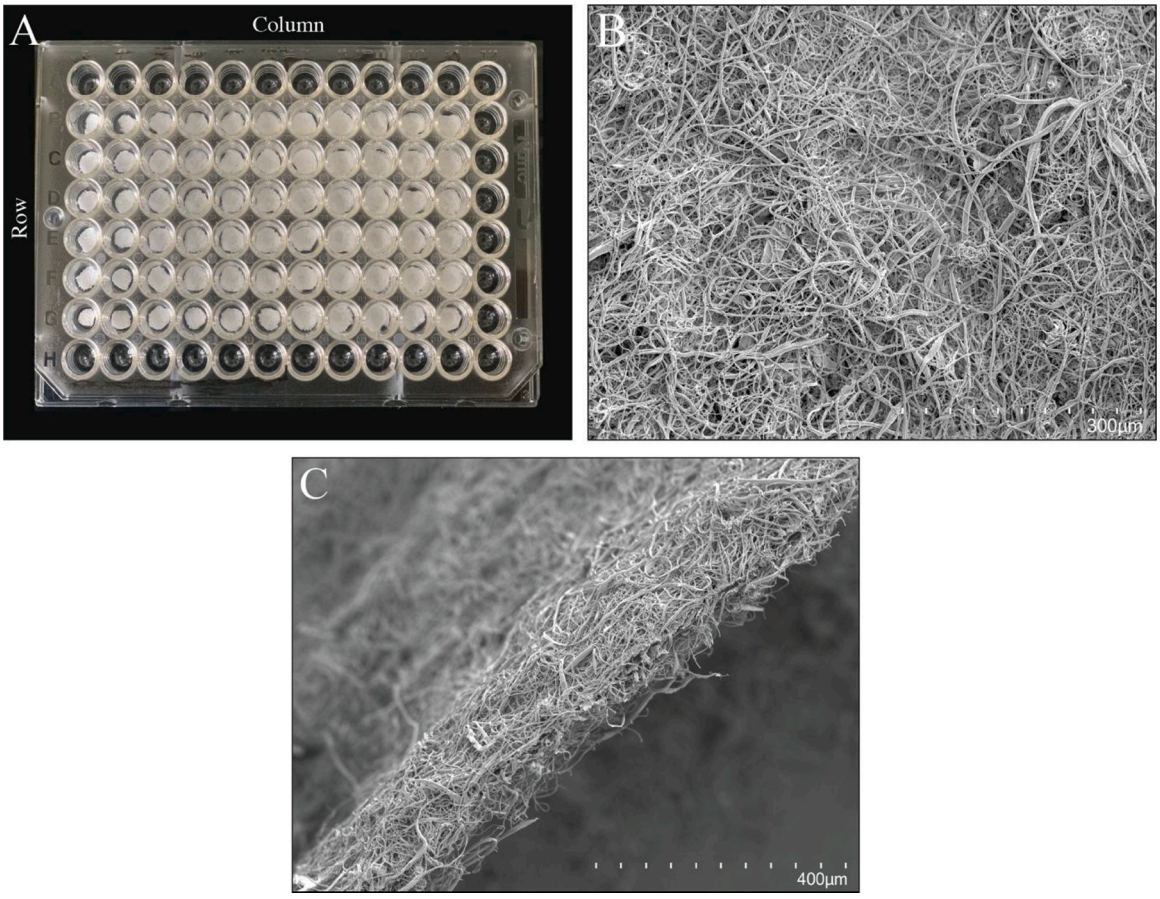

Fig. 1. Image of the 96-well plate with 3D PCL-based fibre network (A), a scanning electron microscopy image of the top view (B), and cross-sectional view (C) of the fibre network extracted from a well. Scale bars are 300 µm (B) and 400 µm (C). Images B and C are representative of 3 replicates.

ingrowth. JIMT-1 cells were observed with mean infiltration depth of 112 ± 8.5 µm (n = 10) in the z direction into the HTS 3D fibre network both in hypoxia and normoxia. This depth of cellular growth is lower than the filter thickness shown in Fig. 1C, however, there is some compression by the cells and handling of the fibre networks during staining as we have observed previously [14].

3.3. Toxicity of anti-cancer compounds in 2D and 3D cultures

Figs. 4 and 5 show dose response curves of combined data deduced from three independent experiments for HDFs and JIMT-1 cells, respectively. The cells were treated with different concentrations of SAEC or paclitaxel grown in normoxia or hypoxia. The individual dose response curves from the independent experiments are found in Supplementary Figures S1 and S2. An inhibitory concentration 50 (IC_{50}) was extracted from each independent dose response curve, and the means and SEM are shown in Table 1 for SAEC and Table 2 for paclitaxel. The dose response curves show that both treatments resulted in dose dependent decrease in MTT reduction in both cell lines when grown 2D and 3D (except for SAEC-treated HDFs in hypoxia) (Figs. 4 and 5). All curves obtained from 2D cultures are found to the left of curves obtained from 3D cultures implicating lower toxicity of the compounds on cells in 3D cultures.

Table 1 shows that the IC_{50} values for SAEC are higher when the cells are cultured in 3D compared to 2D cultures. Notable is also that the toxicity of SAEC is higher in normoxia compared to hypoxia with the exception of JIMT-1 cells in 2D. Thus, SAEC is more toxic to cells grown in 2D cultures compared to cells grown in 3D cultures.

Table 2 shows that the IC_{50} values for paclitaxel are higher when the cells are cultured in 3D compared to 2D and that the IC_{50} values are higher in hypoxia compared to normoxia. Thus, paclitaxel is more toxic to cells cultured in 2D compared to cells cultured in 3D.

4. Discussion

Performing 2D dose response assays is a routine procedure in most laboratories working with chemicals to deduce dose ranges of toxicity in various contexts from basic research to chemical safety. Most commonly so far, commercially available 2D 96-well plates are used for dose response assays using various end point read outs based *e.g.* on protein content (sulforhodamine blue assay), cellular metabolism (MTT, AlamarBlue™, and WST assays), or lysosomal activity (neutral red uptake). In an HTS industrial contexts, dose response assays are performed efficiently by using 384- or 1536-well plates designed and manufactured for robotic handling. However, the large failure rate of 2D-based data to predict pre-clinical compound efficiency has called to mind that 2D cell cultures actually do not mimic 3D *in vivo* physiology. Thus, the past decades have witnessed significant efforts toward the development of 3D cell cultures that hopefully better mimic tissue-specific architecture with multiple cell types and unique ECM, which consider mechanical and biochemical cues, cell-to-cell, and cell-to-matrix interactions. These 3D models should have the capacity to be reproducibly used in small and large laboratories and importantly can be applicable to HTS settings. They should also be used with a minimum of animal-derived products in the wake of governments suggesting the reduction of animal experiments. Here, we present the development of an HTS-compatible 3D PCL-based 96-well plate that can be produced in any standard laboratory with access to electrospinning equipment to fabricate PCL fibres or possibility to purchase commercially available PCL fibres.

In the process of producing the 3D fibre network, we observed that it

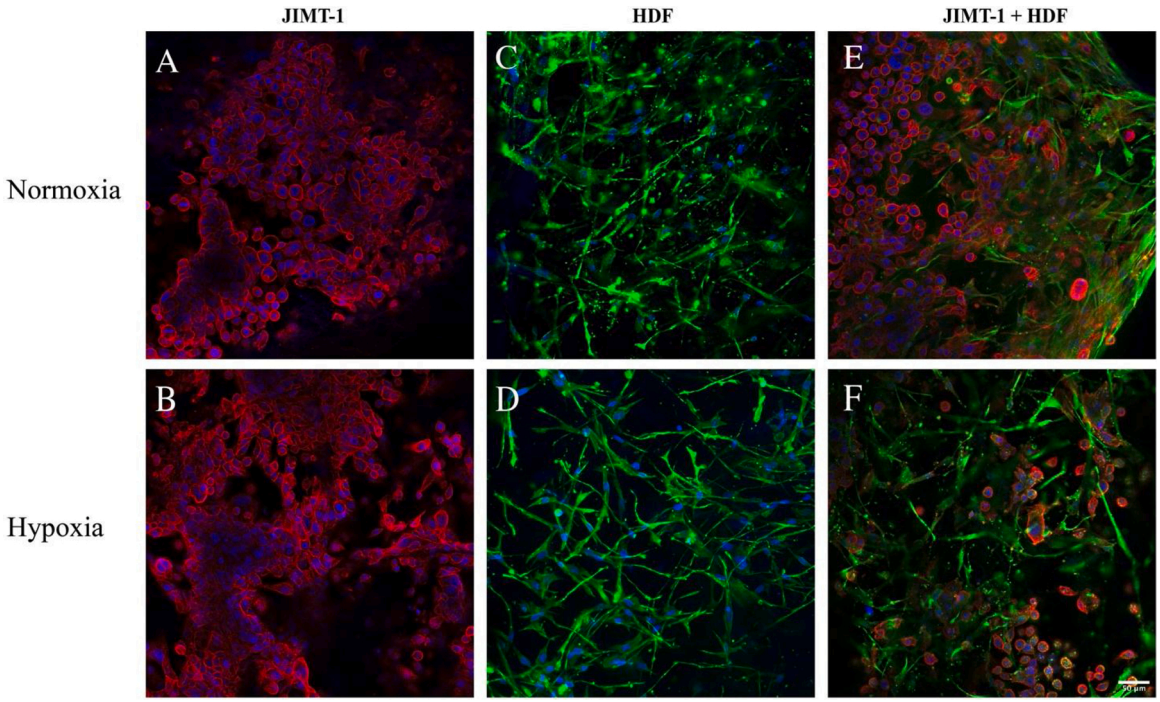

Fig. 2. Single confocal microscopy plane images taken horizontally in the centre of 3D mono-cultures of JIMT-1 cells (A,B), HDFs (C,D), and co-cultures of both cell lines (E,F) incubated in normoxia (18 % O_2) (A,C,E) or hypoxia (1 % O_2) (B,D,F). All the cultures were incubated in 3D 96-well plates for 96 h under normoxic or hypoxic (24 h of normoxia and 72 h of hypoxia,) conditions. The PCL-fibre networks were then extracted from the wells and the cultures were fixed in 3.7 % formaldehyde and labelled to visualize CD44 (red), vimentin (green), and cell nuclei (blue). All images are representative of 3 independent experiments. Scale bar indicates 50 μm.

was important to keep the fibres at a temperature lower than or close to the PCL polymer glass transition temperature (−60 °C) in order to prevent the fibres to lump together due to their "stickiness" at higher temperatures [23]. Thus, the aligned PCL fibres were kept at −80 °C throughout the preparation procedures before being submerged into the ethanol/water solution at −80 °C (on dry ice). Then, the cold solution was transferred into the sterilized and cooled mixer (by adding liquid nitrogen) kept in a laminar flow hood bench. To ensure the solution stayed below −60 °C during the cutting of the PCL fibres into small pieces, liquid nitrogen was added. However, liquid nitrogen addition has to be carefully controlled to prevent complete freezing of the mixture, which hinders the cutting process by the mixer. The obtained homogenous PCL solution can then be pipetted at micro volumes into 96-well plates using a multichannel pipette. It is preferable to pipette the PCL solution into the wells of 96-well plates while the solution is still cold. The 96-well plates with the PCL solution were allowed to reach room temperature (1 h) before thermally cross-linking. The cross-linking time of 7 min at 59 °C was found to be optimal for preparation of 3D fibre networks with stability to allow extraction from the wells for visualization by SEM. Longer cross-linking times resulted in agglomeration of the fibres into a dense structure. The 3D 96-well plates were subjected to O_2 plasma treatment before sterilization, cell seeding, and compound treatment as described in Materials and Methods section. For evaluation of the dose response testing, we used the MTT colorimetric assay which is based on the reduction of MTT by cellular metabolism resulting in the formation of insoluble formazan in the cells [24]. As each cell is assumed to reduce the same amount of MTT, the total amount of formazan produced should be proportional to the cell number. To be able to obtain data from the formazan crystals, the medium is removed and 100 % DMSO is added to the wells to dissolve the formazan into a coloured solution. For 2D experiments, the cultures are incubated for approximately 15 min for cell lysis in order to obtain a homogenous purple blue solution for measurement of absorption in a spectrophotometer. However, we found that 3D cultures need to be incubated for 2 h to ensure complete cell lysis and formazan solubilisation. In addition, it is not possible to measure absorption directly in the round-bottomed 3D 96-well plates as the filters disturbed the light path of the spectrophotometer. Thus, the DMSO solution was transferred to new flat-bottomed 96-well plates before absorbance measurements in a spectrophotometer. In conclusion, it should be feasible for any laboratory to produce these 3D 96-well plates for screening of chemical compounds. We believe this system can be adapted to 384-and 1536-well microtiter plates as well as it is possible to pipette small volumes of the PCL fibre solution.

SEM imaging shows that the PCL fibre size and the porosity of the 3D filters are compatible with the PCL fibres in a number of published papers [13,14,25–27]. We show confocal microscopy images of the cells grown in the fibre network of the 3D 96-well plate (Figs. 2 and 3). The cells grow in a 3D manner similar to what we have observed before in another type of 3D PCL-based culture set up [14]. Thus, with the confirmation of a 3D growth of cells in the 96-well plates using z stack measurements, we further proceeded to treat the JIMT-1 and HDF mono-cultures with compounds and compared the toxicity in 2D and 3D cultures incubated in normoxia and hypoxia.

We opted to choose paclitaxel since it is a well-established chemotherapeutic drug used in the clinic for the treatment of different cancers [28]. There are also many studies comparing paclitaxel toxicity in 2D and 3D cultures [29–32]. Furthermore, several other studies investigated the potency of paclitaxel in 2D cultures under normoxic and hypoxic conditions [33,34]. In addition, we used the experimental salinomycin analogue SAEC in our study [19]. Salinomycin was identified in HTS 2D cultures for selective breast cancer stem cell (CSC) inhibition [35] and has subsequently been shown to effectively inhibit CSCs and induce apoptosis in many cancer types [36]. Since the discovery of salinomycin, extensive research has been ongoing to chemically modify salinomycin to increase bioactivity. SAEC belongs to a group of the most bioactive and potent semi synthetic salinomycin analogues so far obtained by selective chemical modification strategies [18,19]. The JIMT-1 cell line was chosen on the basis of our prior long-time

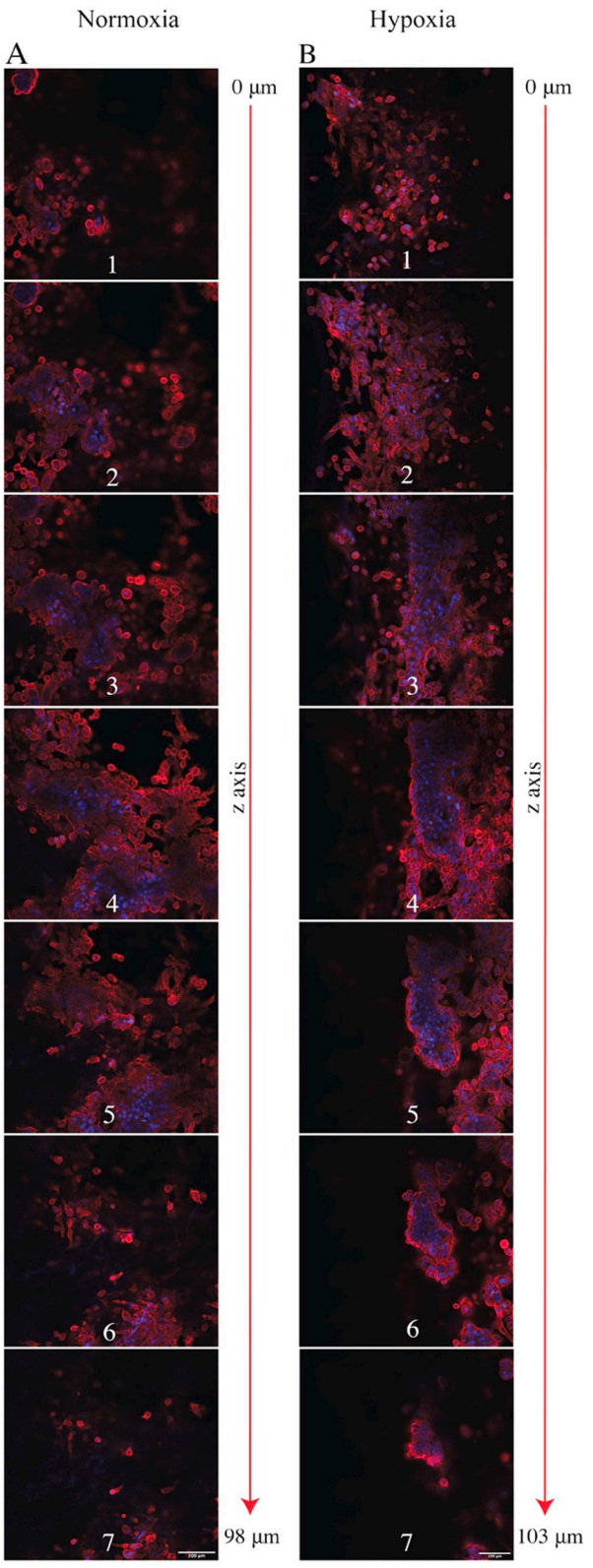

Fig. 3. Focus stacking images of 3D cultures of JIMT-1 cells in normoxia (18 % O_2) (A) and hypoxia (1 % O_2) (B). The cultures were fixed in 3.7 % formaldehyde after 96 h incubation (for the hypoxic culture, 24 h of normoxia and 72 h of hypoxia) and labelled to visualize CD44 (red) and cell nuclei (blue). Seven confocal plane images were obtained showing the depth of 98 µm and 103 µm in representative cultures incubated in normoxia and hypoxia, respectively. Scale bars are 100 µm.

experimental knowledge of this cell line in the search for new anti-cancer chemicals in 2D dose response testing [18,37–39]. We have established 3D mono-cultures of the JIMT-1 cells and HDFs [14] as well as co-cultures of the two cell lines and investigated toxicity of paclitaxel and SAEC. However, the 3D cultures used in previous studies are not scalable to microtiter plates and therefore cannot be used for dose response testing which contributed to the need of developing the 3D HTS-based culture plates presented here.

Here, we show dose response curves obtained using our 3D PCL-based 96-well plates and compare them with dose response curves obtained using conventional 2D 96-well plates. We have previously found an IC_{50} of 90 ± 0.02 nM for JIMT-1 cells in 2D cultures incubated in normoxia treated with SAEC [18]. However, we obtained a higher IC_{50} value of 119.5 ± 13.2 nM in this work, showing slightly lower inhibitory effect compared to the previous investigation. We speculate that the differences in these IC_{50} values (which is small) is a result of different sera used in the two studies. In the former study, the most widely used serum supplement, fetal bovine serum (FBS) was used, while we currently have switched to DHHS in compliance with the 3R to reduce the use of products derived by causing animal suffering. It is no doubt a fact that the use of FBS raises serious scientific and ethical concerns [40]. SAEC was less toxic to JIMT-1 cells in 3D culture compared to 2D cultures, which was specifically evident when the cultures were incubated in hypoxia where an IC_{50} was not obtained within the dose range studied. Altogether, these data show the importance of investigating compound toxicity in 3D as well as in both normoxic and hypoxic environments. It is well known that tumours have areas of hypoxia and that these areas show lower sensitivity to drug treatment [16,17; Trédan et al., 2007]. We have shown that JIMT-1 cells in 2D proliferate slower in hypoxia compared to normoxia, which may also contribute to the decreased sensitivity to paclitaxel treatment of JIMT-1 cells incubated in 3D in hypoxia compared to normoxia [41].

Regarding paclitaxel sensitivity, the cells incubated in 2D were more sensitive than cells incubated in 3D. This has also been found by others comparing toxicity of paclitaxel in cancer cells grown in 2D and 3D, using 3D model systems that deviate from ours such as the use of a hydrogel matrix and multicellular spheroid cultures [29–32]. Souza et al. [31] evaluated paclitaxel chemoresistance in cancer cell lines using magnetic 3D bioprinting to induce the cells to form spheroids in medium supplemented with FBS. Loessner et al. [29] encapsulated cells in polyethylene glycol-based hydrogel surrounded by medium containing FBS resulting in the formation of spheroids. Nirmalanandhan et al. [30] seeded cells in rat tail type I collagen hydrogel in FBS-supplemented medium to obtain spheroids. Imamura et al. [31] suspended cells in FBS-supplemented medium in specifically designed 96-well plates which promoted formation of spheroids. We have not found any studies comparing toxicity of paclitaxel in 2D and 3D in hypoxia as presented here. However, there are studies comparing toxicity of paclitaxel in 2D in cultures incubated in normoxia or hypoxia [33,34]. In line with our study, they also show that paclitaxel is less toxic in hypoxia compared to normoxia. It has previously been shown that hypoxia induces resistance against various agents such as paclitaxel and decreases the efficacy of paclitaxel in breast cancer cells [42–45]. The IC_{50} values obtained here for paclitaxel-treated HDFs grown in 2D, is similar to that obtained in other studies [46,47].

Here, we present data showing a decreased toxicity of two cytotoxic compounds when cells are grown in 3D compared to 2D which is similar to what has been reported by many groups when comparing toxicity in 3D using different model systems and conventional 2D cell culturing. It should be kept in mind that most 3D cell culturing implies an increased surface area to which the compound used for treatment can bind, thus decreasing the true free treatment concentration that reaches the cells [48]. The same holds true when comparing concentrations used in cell cultures and doses applied to tumour bearing animals [48]. Thus, data from 3D cell culturing may better reflect doses that should be used when testing potential anti-cancer compounds in tumour bearing animals.

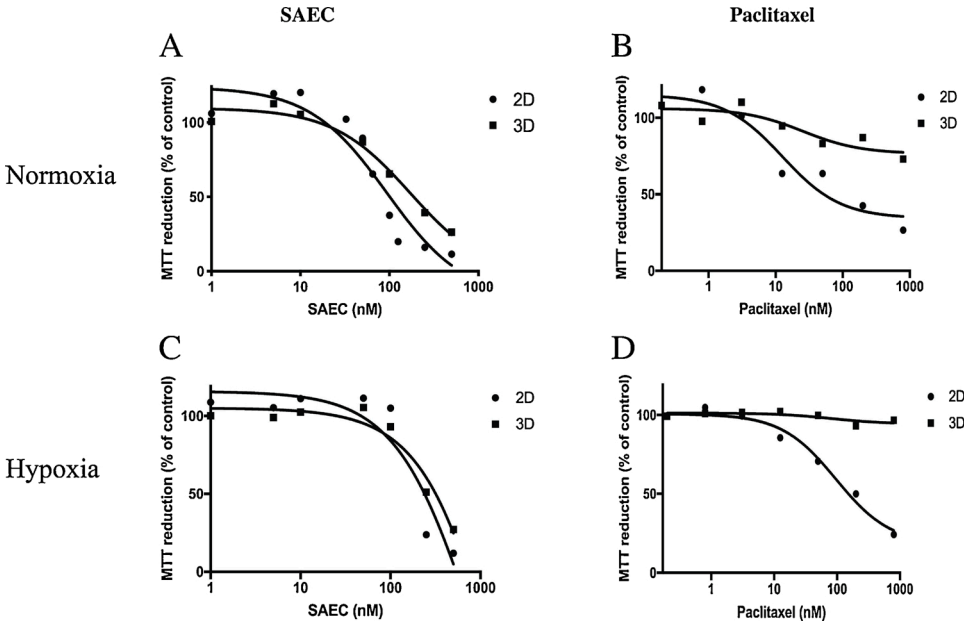

Fig. 4. Dose response curves for human dermal fibroblasts in 2D and 3D cultures treated with SAEC or paclitaxel and incubated in normoxia (18 % O_2) or hypoxia (1 % O_2). The cells were seeded and incubated for 24 h in normoxia to allow cell attachment before addition of compound at the indicated concentrations. Cultures to be incubated in hypoxia were then transferred to the hypoxia station. After 72 h of incubation, the toxicity was evaluated using an MTT assay. The curves are drawn in GraphPad Prism 8 using all data from three independent experiments with n = 12-18 for each data point in the figure. Individual dose response curves for each of the three experiments are found in Supplementary Figures S1 and S2.

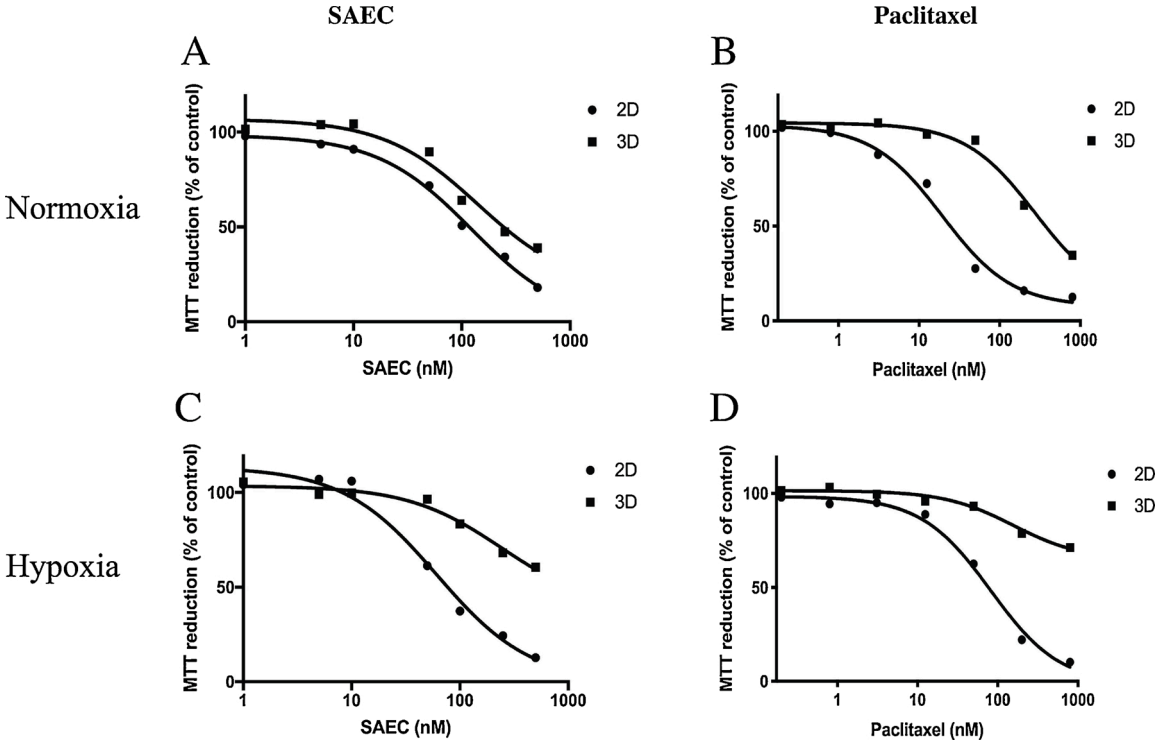

Fig. 5. Dose response curves for JIMT-1 breast cancer cells in 2D and 3D cultures treated with SAEC or paclitaxel and incubated in normoxia (18 % O_2) or hypoxia (1 % O_2). The cells were seeded and incubated for 24 h in normoxia to allow cell attachment before addition of compound at the indicated concentrations. Cultures to be incubated in hypoxia were then transferred to the hypoxia station. After 72 h of incubation, the toxicity was evaluated using an MTT assay. The curves are drawn in GraphPad Prism 8 using all data from three independent experiments with n = 12-18 for each data point in the figure. Individual dose response curves for each of the three experiments are found in Supplementary Figures S1 and S2.

This notion however, needs careful investigation of the pharmacokinetics of a compound *i.e.* comparing the distribution in different compartments in a 3D cell culture and in a tumour bearing animal. A vital difference between a cell culture and an animal that will affect pharmacokinetics is the lack of biotransformation in the former, which, however, can be included in testing of chemicals.

5. Conclusions

In conclusion, we here present the fabrication and use of a unique 3D 96-well PCL-based plate that can be used for screening of compounds. Commercially available 3D 96-well plates based on PCL or other polymers are highly costly which may explain why they have not been used extensively in 2D/3D drug efficacy investigations so far. Our 3D 96-well plate can be produced in any laboratory setting with minimum level of

Table 1
IC_{50} values in nM concentrations for HDFs and JIMT-1 cells grown in 2D or 3D cultures treated with SAEC incubated in normoxia (18 % O_2) or hypoxia (1 % O_2)[a].

	HDF		JIMT-1	
	2D	3D	2D	3D
Normoxia	97.7 ± 11.8 [b]	150.3 ± 34.4	119.5 ± 13.2	271.3 ± 52.2
Hypoxia	239.3 ± 6.2	316.2 ± 35.1	80.4 ± 13.3	NA [c]

[a] The data is derived from the dose response curves found in Supplementary Figures S1 and S2.
[b] Mean of three independent experiments ± SEM.
[c] NA, not applicable within the dose range studied.

Table 2
IC_{50} values in nM concentrations for HDFs and JIMT-1 cells grown in 2D or 3D cultures treated with paclitaxel incubated in normoxia (18 % O_2) or hypoxia (1 % O_2). [a].

	HDF		JIMT-1	
	2D	3D	2D	3D
Normoxia	61.7 ± 13.8 [b]	NA	49.9 ± 14.8	332.9 ± 95.6
Hypoxia	157.1 ± 34.0	NA	74.8 ± 18.6	NA[c]

[a] The data is derived from the dose response curves found in Supplementary Figures S1 and S2.
[b] Mean of three independent experiments ± SEM.
[c] NA, not applicable within the dose range studied.

expertise which we find specifically important in research groups with limited funding. The future development of 3D plates for drug screening should be based on compliance with the 3R to reduce the use of animal derived products such as collagen and Matrigel™ as well as FBS as medium supplement. As already stated, we have replaced FBS with DHHS in the growth medium and we have an ongoing investigation to use totally defined medium in our 3D culturing studies (unpublished results). As the fibre network can be extracted from the wells of 96-well plates and used for co-culturing, more advanced studies than basic dose response assays *e.g.* cell-cell interactions, cell-ECM interactions, and molecular studies can be performed efficiently and to a low cost. Further studies are needed to investigate if 3D co-cultures can be used for cytotoxicity testing. Here, the challenge is to have an HTS compatible system to distinguish between effects on cancer cells and fibroblasts.

Authors statements

Conceptualisation: AMP, SO. Data curation: AMP, SO. Formal analysis: AMP, SO. Funding acquisition: AMP, SO. Investigation: AMP, SO. Methodology: AMP, SO. Project administration: AMP, SO. Resources: SO. Supervision: SO. Validation: AMP, SO. Visualization: AMP. Writing original draft: SO. Review and editing: AMP, SO.

Declaration of Competing Interest

The authors Atena Malakpour-Permlid and Stina Oredsson declare that they have no known competing financial interests or personal relationships that could have appeared to influence the work reported in this paper.

Acknowledgements

The authors are grateful to the Swedish Fund for Research Without Animal Experiments (Forska Utan Djurförsök), Carolina Le Prince with the "Kalenderflickorna", and the Royal Physiographical Society in Lund for funding of this work. The funding bodies plays no role in the design of the study, collection, analysis, interpretation of data, and writing of manuscript. The authors thank Per Fredrik Johansson for the use of the electrospinning system.

Appendix A. Supplementary data

Supplementary material related to this article can be found, in the online version, at doi:https://doi.org/10.1016/j.toxrep.2021.03.015.

References

[1] D.A. Pereira, J.A. Williams, Origin and evolution of high throughput screening, Brit J Pharmacol 152 (2007) 53–61, https://doi.org/10.1038/sj.bjp.0707373.
[2] E. Cukierman, R. Pankov, D.R. Stevens, et al., Taking cell-matrix adhesions to the third dimension, Science 294 (2001) 1708–1712, https://doi.org/10.1126/science.1064829.
[3] M.J. Bissell, A. Rizki, I.S. Mian, Tissue architecture: the ultimate regulator of breast epithelial function, Curr. Opin. Cell Biol. 15 (2003) 753–762, https://doi.org/10.1016/j.ceb.2003.10.016.
[4] Y. Fang, R.M. Eglen, Three-dimensional cell cultures in drug discovery and development, Slas discovery: Adv. Life Sci. R&D 22 (2017) 456–472.
[5] R. Edmondson, J.J. Broglie, A.F. Adcock, et al., Three-dimensional cell culture systems and their applications in drug discovery and cell-based biosensors, Assay Drug Dev Tech 12 (2014) 207–218, https://doi.org/10.1089/adt.2014.573.
[6] M.P. Nikolova, M.S. Chavali, Recent advances in biomaterials for 3D scaffolds: a review, Bioactive Mat 4 (2019) 271–292, https://doi.org/10.1016/j.bioactmat.2019.10.005.
[7] P. Baillargeon, J. Shumate, S. Hou, et al., Automating a magnetic 3D spheroid model technology for high-throughput screening, SLAS Technol.: Translating Life Sci. Innovation 24 (2019) 420–428, https://doi.org/10.1177/2472630319854337.
[8] R. Lehmann, C. Gallert, T. Roddelkopf, et al., Biomek cell workstation: a flexible system for automated 3D cell cultivation, J. Lab. Autom. 21 (2016) 568–578, https://doi.org/10.1177/2211068215594580.
[9] L. Li, D.V. LaBarbera, 3D High-content screening of organoids for drug discovery, Compr Med Chem III (2017) 388–415, https://doi.org/10.1016/B978-0-12-409547-2.12329-7.
[10] G. Mehta, A.Y. Hsiao, M. Ingram, et al., Opportunities and challenges for use of tumor spheroids as models to test drug delivery and efficacy, J Cont Rel: Official J Contr Release Society 164 (2012) 192–204, https://doi.org/10.1016/j.jconrel.2012.04.045.
[11] N. Chaicharoenaudomrung, P. Kunhorm, P. Noisa, Three-dimensional cell culture systems as an in vitro platform for cancer and stem cell modelling, World J. Stem Cells 11 (2019) 1065–1083, https://doi.org/10.4252/wjsc.v11.i12.1065.
[12] E.A. Aisenbrey, W.L. Murphy, Synthetic alternatives to matrigel, Nat. Rev. Mater. 5 (2020) 539–551, https://doi.org/10.1038/s41578-020-0199-8.
[13] A. Jakobsson, M. Ottosson, M.C. Zalis, et al., Three-dimensional functional human neuronal networks in uncompressed low-density electrospun fiber scaffolds, Nanomedicine 13 (2017) 1563–1573, https://doi.org/10.1016/j.nano.2016.12.023.
[14] A. Malakpour-Permlid, P. Roci, E. Fredlund, et al., Unique animal friendly 3D culturing of human cancer and normal cells, Toxicol. Vitr. 60 (2019) 51–60, https://doi.org/10.1016/j.tiv.2019.04.022.
[15] A. Malakpour-Permlid, I. Buzzi, C. Hegardt, et al., Identification of extracellular matrix proteins secreted by human dermal fibroblasts cultured in 3D electrospun scaffolds, Sci. Rep. (2021) in press.
[16] B.A. Teicher, Hypoxia and drug resistance, Cancer Metastasis Rev. 13 (1994) 139–168, https://doi.org/10.1007/BF00689633.
[17] S. Strese, M. Fryknäs, R. Larsson, et al., Effects of hypoxia on human cancer cell line chemosensitivity, BMC Cancer 13 (2013) 1–11, https://doi.org/10.1186/1471-2407-13-331.
[18] B. Borgström, X. Huang, M. Pošta, et al., Synthetic modification of salinomycin: selective O-acylation and biological evaluation, Chem. Commun. 49 (2013) 9944–9946, https://doi.org/10.1039/C3CC45983G.
[19] X. Huang, B. Borgström, S. Kempengren, et al., Breast cancer stem cell selectivity of synthetic nanomolar-active salinomycin analogs, BMC Cancer 23 (2016) 145, https://doi.org/10.1186/s12885-016-2142-3.
[20] R.H. Wenger, Kurtcuoglu Kurtcuoglu, C.C. Scholz,, et al., Frequently asked questions in hypoxia research, Hypoxia (2015), https://doi.org/10.2147/HP.S92198.
[21] M. Vaapil, K. Helczynska, R. Villadsen, et al., Hypoxic conditions induce a cancer-like phenotype in human breast epithelial cells, PLoS One 7 (2012) e46543, https://doi.org/10.1371/journal.pone.0046543.
[22] H. Jaganathan, J. Gage, F. Leonard, et al., Three-dimensional in vitro co-culture model of breast tumor using magnetic levitation, Sci. Rep. 4 (1) (2015), https://doi.org/10.1089/ten.tec.2019.0122.
[23] J.C. Middleton, A.J. Tipton, Synthetic biodegradable polymers as orthopedic devices, Biomaterials 21 (2000) 2335–2346, https://doi.org/10.1016/s0142-9612(00)00101-0.
[24] S.A. Ahmed, R.M. Gogal Jr, J.E. Walsh, A new rapid and simple non-radioactive assay to monitor and determine the proliferation of lymphocytes: an alternative to H3-thymidine incorporation assay, J Immunol Meth 170 (1994) 211–224, https://doi.org/10.1016/0022-1759(94)90396-4.
[25] S. Saha, X. Duan, L. Wu, et al., Electrospun fibrous scaffolds promote breast cancer cell alignment and epithelial-mesenchymal transition, Langmuir: the ACS J Surfaces Colloids 28 (2012) 2028–2034, https://doi.org/10.1021/la203846w.

[26] X.Duan Feng, P.K. Lo, et al., Expansion of breast cancer stem cells with fibrous scaffolds, Integrative Biol 5 (2013) 768–777, https://doi.org/10.1039/c3ib20255k.
[27] M. Rabionet, M. Yeste, T. Puig, et al., Electrospinning PCL scaffolds manufacture for three-dimensional breast cancer cell culture, Polymers 9 (2017) 328, https://doi.org/10.3390/polym9080328.
[28] A.M. Barbuti, Z.S. Chen, Paclitaxel through the ages of anticancer therapy: exploring its role in chemoresistance and radiation therapy, Cancers 7 (2015) 2360–2371, https://doi.org/10.3390/cancers7040897.
[29] D. Loessner, K.S. Stok, M.P. Lutolf, et al., Bioengineered 3D platform to explore cell–ECM interactions and drug resistance of epithelial ovarian cancer cells, Biomaterials 3 (2010) 8494–8506, https://doi.org/10.1016/j.biomaterials.2010.07.064.
[30] V.S. Nirmalanandhan, A. Duren, P. Hendricks, et al., Activity of anticancer agents in a three-dimensional cell culture model, Assay Drug Devt. Technol. 8 (2010) 581–590, https://doi.org/10.1089/adt.2010.0276.
[31] Y. Imamura, T. Mukohara, Y. Shimono, et al., Comparison of 2D- and 3D-culture models as drug-testing platforms in breast cancer, Oncol Reports 33 (2015) 1837–1843, https://doi.org/10.3892/or.2015.3767.
[32] A.G. Souza, I.B.B. Silva, E. Campos-Fernandez, et al., Comparative assay of 2D and 3D cell culture models: proliferation, gene expression and anticancer drug response, Current Pharmaceut Design 24 (2018) 1689–1694, https://doi.org/10.2174/1381612824666180404152304.
[33] S. Koch, F. Mayer, F. Honecker, et al., Efficacy of cytotoxic agents used in the treatment of testicular germ cell tumours under normoxic and hypoxic conditions *in vitro*, Br. J. Cancer Suppl. 89 (2003) 2133–2139, https://doi.org/10.1038/sj.bjc.6601375.
[34] L. Huang, Q. Ao, Q. Zhang, et al., Hypoxia induced paclitaxel resistance in human ovarian cancers via hypoxia-inducible factor 1α, J. Cancer Res. Clin. Oncol. 136 (2010) 447–456, https://doi.org/10.1007/s00432-009-0675-4.
[35] P.B. Gupta, T.T. Onder, G. Jiang, et al., Identification of selective inhibitors of cancer stem cells by high-throughput screening, Cell 138 (2009) 645–659, https://doi.org/10.1016/j.cell.2009.06.034.
[36] M. Antoszczak, A comprehensive review of salinomycin derivatives as potent anticancer and anti-CSCs agents, Eur. J. Med. Chem. 166 (2019) 48–64, https://doi.org/10.1016/j.ejmech.2019.01.034.
[37] W.S. Sotillo, R. Villagomez, S. Smiljanic, et al., Anti-cancer stem cell activity of a sesquiterpene lactone isolated from Ambrosia arborescens and of a synthetic derivative, PLoS One 12 (2017) e0184304, https://doi.org/10.1371/journal.pone.0184304.
[38] N. Tuasha, D. Seifu, E. Gadisa, et al., Cytotoxicity of selected Ethiopian medicinal plants used in traditional breast cancer treatment against breast-derived cell lines, J. Med Plants Res 13 (2019) 188–198, https://doi.org/10.5897/JMPR2019.6772.
[39] M. Lozano, W. Soria, G.R. Almanza, et al., Selective cytotoxicity of damsin derivatives in breast cancer cells, J. Adv. Pharm. Sci. Tech 2 (2019) 23–37, https://doi.org/10.14302/issn.2328-0182.japst-19-2759.
[40] C.E. Jochems, J.B. Van Der Valk, F.R. Stafleu, et al., The use of fetal bovine serum: ethical or scientific problem? ATLA 30 (2002) 219–227, https://doi.org/10.1177/026119290203000208.
[41] S. Kamlund, D. Strand, B. Janicke, et al., Influence of salinomycin treatment on division and movement of individual cancer cells cultured in normoxia or hypoxia evaluated with time-lapse digital holographic microscopy, Cell Cycle 16 (2017) 2128–2138, https://doi.org/10.1080/15384101.2017.1380131.
[42] P. Vaupel, D.K. Kelleher, M. Hoeckel, Oxygen status of malignant tumors: pathogenesis of hypoxia and significance for tumor therapy, Sem Oncol 28 (2001) 29–35, https://doi.org/10.1016/s0093-7754(01)90210-6.
[43] M. Hoeckel, P. Vaupel, Tumor hypoxia: definitions and current clinical, biologic, and molecular aspects, J. Natl. Cancer Inst. Monographs 93 (2001) 266–276, https://doi.org/10.1093/jnci/93.4.266.
[44] X.L. Dong, P.F. Xu, C. Miao, et al., Hypoxia decreased chemosensitivity of breast cancer cell line MCF-7 to paclitaxel through cyclin B1, Biomed. Pharmacother. 66 (2012) 70–75, https://doi.org/10.1016/j.biopha.2011.11.016.
[45] A. Notte, N. Ninane, T. Arnould, et al., Hypoxia counteracts taxol-induced apoptosis in MDA-MB-231 breast cancer cells: role of autophagy and JNK activation, Cell Death Dis. 4 (2013) e638, https://doi.org/10.1038/cddis.2013.167.
[46] F.M. Van Bockxmeer, C.E. Martin, D.E. Thompson, et al., Taxol for the treatment of proliferative vitreoretinopathy, Invest. Ophthalmol. Vis. Sci. 26 (1985) 1140–1147, https://doi.org/10.1007/BF00918482.
[47] M. Kalinowski, H. Alfke, B. Kleb, et al., Paclitaxel inhibits proliferation of cell lines responsible for metal stent obstruction: possible topical application in malignant bile duct obstructions, Invest. Radiol. 37 (2002) 399–404, https://doi.org/10.1097/00004424-200207000-00007.
[48] J. Kisitu, S. Hougaard Bennekou, M. Leist, Chemical concentrations in cell culture compartments (C5) – concentration definitions, ALTEX - Alternatives to animal experimentation 36 (2019) 154–160, https://doi.org/10.14573/altex.1901031.